

Light-induced reorientation and birefringence in polymeric dispersions of nano-sized crystals

Roberto Termine,² Iolinda Aiello,¹ Nicolas Godbert,¹ Mauro Ghedini¹ and Attilio Golemme^{1,*}

¹ LASCAMM, CR-INSTM Unità della Calabria, Laboratorio Regionale Licryl, CNR-INFM, Centro di Eccellenza CEMIF.CAL Dipartimento di Chimica, Università della Calabria, 87036 Rende (Italy)

² Laboratorio Regionale Licryl, CNR-INFM, Centro di Eccellenza CEMIF.CAL, Università della Calabria, 87036 Rende (Italy)

*Corresponding author: a.golemme@unical.it

Abstract: Nanocrystals (50-250 nm) of a Palladium complex within a polyisobutylmethacrylate matrix were prepared by a phase separation method. In these dispersions, a light-induced birefringence with $\Delta n \sim 10^{-3}$ was induced, without the application of an electric field. This effect was related to the photoconducting properties of the dispersion. Evidence for charge photogeneration without any applied field was obtained. The photorefractive behaviour of the material confirmed that the nanocrystals reorientation is a consequence of photoconducting properties. A light-generated electric field $E \sim 3 \text{ V}/\mu\text{m}$ was estimated. These results illustrate the potential of materials with a nano-crystalline dispersion morphology as light-responsive media.

©2008 Optical Society of America

OCIS codes: (160.4236) Nanomaterials; (160.5335) Photosensitive Materials; (160.4890) Organic Materials; (160.5335) Photorefractive Materials; (160.5140) Photoconductive materials; (160.4890) Semiconductors Materials.

References and links

1. F. Giacalone and N. Martin, "Fullerene Polymers: Synthesis and Properties," *Chem. Rev.* **106**, 5136-5190 (2006).
2. H. Akiyama and N. Tamaoki, "Synthesis and Photoinduced Phase Transitions of Poly(*N*-isopropylacrylamide) Derivative Functionalized with Terminal Azobenzene Units," *Macromolecules* **40**, 5129-5132 (2007).
3. H. Yu, S. Asaoka, A. Shishido, T. Iyoda, and T. Ikeda, "Photoinduced Nanoscale Cooperative Motion in a Well-Defined Triblock Copolymer," *Small* **3**, 768-771 (2007).
4. A. G. Griesbeck, N. Hoffmann, and K.D. Warzecha, "Photoinduced-Electron-Transfer Chemistry: from Studies on PET Processes to Applications in Natural Product Synthesis," *Acc. Chem. Res.* **40**, 128-140 (2007).
5. W. Wang, K. Allaart, and D. Lenstra, "Photo-Induced Birefringence in Semiconductors Compared with Optical Fibers," *Opt. Commun.* **278**, 395-401 (2007).
6. G. Boudebs and C. B. de Araújo, "Characterization of Light-Induced Modification of the Nonlinear Refractive Index Using a One-Laser-Shot Nonlinear Imaging Technique," *Appl. Phys. Lett.* **85**, 3740-3742 (2004).
7. P. Yeh, *Introduction to Photorefractive Nonlinear Optics* (Wiley-Interscience, 1993).
8. L. Solymar, D. J. Webb, and A. Grunnet-Jepsen, *The Physics and Applications of Photorefractive Materials* (Oxford UP, 1996).
9. M. Duelli, G. Montemezzani, M. Zgonik, and P. Günter, "Photorefractive Memories for Optical Processing," in *Photorefractive Materials and their Applications 3: Applications*, P. Günter, J. P. Huignard, eds. (Springer, 2007), pp. 77-134.
10. P. Dean, M. R. Dickinson, and D. P. West, "Full-Field Coherence-Gated Holographic Imaging through Scattering Media Using a Photorefractive Polymer Composite Device," *Appl. Phys. Lett.* **85**, 363-365 (2004).
11. O. Ostroverkhova and W. E. Moerner, "Organic Photorefractives: Mechanisms, Materials, and Applications," *Chem. Rev.* **104**, 3267-3314 (2004).
12. P. Cheben, F. del Monte, D. J. Worsfold, D. J. Carlsson, C. P. Grover, and J. D. Mackenzie, "A Photorefractive Organically Modified Silica Glass with High Optical Gain," *Nature* **408**, 64-67 (2000).

13. M. M. Huang, Z. J. Chen, J. Shi, S. K. Cao, and Q. H. Gong, "All-Optical Photorefractive Effect in Carbazole-Based Azo-Side Group Polymer," *Chin. Phys. Lett.* **23**, 2468-2471 (2006).
14. P. G. de Gennes, J. Prost, *The Physics of Liquid Crystals* (Oxford UP, 1993).
15. G. P. Wiederrecht, "Photorefractive Liquid Crystals," *Annu. Rev. Mater. Res.* **31**, 139-169 (2001).
16. G. Cipparrone, A. Mazzulla, and P. Pagliusi, "Spatial Periodicity of Photorefractive Orientational Gratings in Dye-Doped Polymer-Liquid Crystal Composite," *Opt. Commun.* **185**, 171-175 (2000).
17. I. Aiello, D. Dattilo, M. Ghedini, and A. Golemme, "Cyclometalated Complexes: A New Class of Highly Efficient Photorefractive Materials," *J. Am. Chem. Soc.* **123**, 5598-5599 (2001).
18. I. Aiello, D. Dattilo, M. Ghedini, A. Bruno, R. Termine, and A. Golemme, "Cyclopalladated Complexes as Photorefractive Materials with High Refractive Index Modulation," *Adv. Mater.* **14**, 1233-1236 (2002).
19. R. Termine, I. Aiello, D. Dattilo, M. Ghedini, and A. Golemme, "Photorefractive Performance Enhancement in Polymer Dispersions of Nanosized Crystalline Domains," *Adv. Mater.* **15**, 723-726 (2003).
20. T. K. Gaylord and M. G. Moharam, "Thin and thick gratings: terminology clarification" *Appl. Opt.* **20**, 3271-3273 (1981).
21. Sandalphon, B. Kippelen, K. Meerholz, and N. Peyghambarian, "Ellipsometric Measurements of Poling Birefringence, the Pockels Effect, and the Kerr Effect in High-Performance Photorefractive Polymer Composites," *Appl. Opt.* **35**, 2346-2354 (1996).
22. Z. Peng, A. R. Gharavi, and L. Yu, "Synthesis and Characterization of Photorefractive Polymers Containing Transition Metal Complexes as Photosensitizer," *J. Am. Chem. Soc.* **119**, 4622-4632 (1997).
23. W. E. Douglas, A. S. Kuzhelev, I. V. Yurasova, O. L. Antipov, L. G. Klapshina, V. V. Semenov, G. A. Domrachev, T. I. Lopatina, and D. M. H. Guy, "Photorefractive properties of new polymer composites incorporating poly[ethynediyl-arylene-ethynediyl-silylene]," *Phys. Chem. Chem. Phys.* **4**, 109-114 (2002).

1. Introduction

The possibility of controlling the properties of materials by using light is one of the most desirable features in a variety of technologies. Light can act through several different effects, such as those triggered by absorption, which include induced reactions [1], phase transitions [2], molecular reorientations and charge-carrier generation [3,4]. Among the properties most affected by light is the refractive index itself, both in linear [5] and in non-linear [6] media, with consequences of particular relevance for photonic and optoelectronic applications.

One important mechanism responsible for light-induced refractive index variations takes advantage of the photoconductive properties of some materials, where charge carriers can be generated upon illumination. If the light intensity is not uniform, when such carriers redistribute in space, an internal electric field can eventually be set up and affect the refractive index via non-linear optical and/or reorientational effects. This phenomenon, called photorefractive (PR) effect [7,8], is important for its applications in optical data storage [9] and image processing [10]. During the last 15 years a variety of organic PR materials have been developed [11], with the aim of substituting inorganic crystals with inexpensive, flexible, light-weight "plastics". The main disadvantage of organic PR materials lays in the high working voltages required for an efficient charge photogeneration and for the reorientation of molecular dipoles. For such reason, the investigation of low-field effects and properties related to both light and electric-field induced modulations of the refractive index are of high interest. Several approaches have been proposed to reduce the intensity of the fields necessary to obtain refractive index variations in organics: such fields are usually very high since their interaction energy with molecular dipoles is well below $k_B T$ at room temperature, even for large molecular dipoles and fields of several tens of V/ μm . In some interesting studies, light-induced conformational motions of chromophores were used in order to assist molecular reorientations [12,13]. In another approach, liquid crystals were used [14-16]: in this case the effect is collective and, given the usual values of the dielectric anisotropies of mesophases, the interaction energies with electric fields are larger than $k_B T$. The same principle was used with dispersions of nanocrystals within organic amorphous photoconductors [17-19]. In this last case, nanocrystals of a cyclopalladated azobenzene complexed to a substituted Schiff base (AZPON) dispersed within an amorphous matrix of polyisobuthylmethacrylate (PIBMA) were obtained by controlled phase separation. The chemical structure of AZPON is shown in Fig. 1. The size of the crystalline domains was

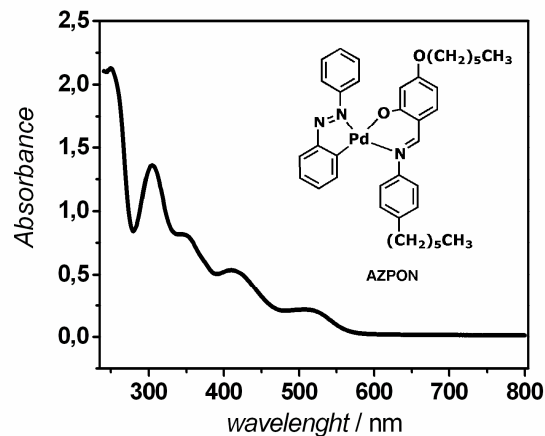


Fig. 1. Absorption spectrum in solution and chemical structure of the cyclopalladated complex AZPON.

in the 50-250 nm range and high electric fields were used to boost photogeneration and reorient the crystalline domains. In this article, experimental results regarding light-induced birefringence and reorientational effects obtained without applying any electric field in similar nanocrystalline dispersions of AZPON will be discussed.

2. Experimental

2.1 Sample preparation

Samples consist of thin films of material sandwiched between two conducting (ITO) glasses. They were prepared by dissolving AZPON and polyisobutylmethacrylate (PIBMA), with a weight ratio AZPON:PIBMA=3:2, in chloroform. After solvent evaporation, the mixture was heated at 130°C for a few minutes and squeezed between the two glasses, controlling the thickness with 50 μm glass spacers. Nano-sized crystalline domains were formed when samples were cooled rapidly to room temperature. The homogeneity of samples and the effective formation of crystalline domains with sizes below the scattering limit in the visible were evaluated by x-ray diffraction, polarized optical microscopy and scanning and transmission electron microscopy.

2.2 Ellipsometric measurements

Light-induced birefringence was measured by an ellipsometric technique, by using light at 633 nm. In such experiments, one beam (intensity around 1.5 W/cm^2) illuminates the sample at normal incidence overlapping with a second weaker probe beam with a 10 $\mu\text{W}/\text{cm}^2$ intensity and at a 45° angle with respect to the sample normal (see Fig. 2). The polarization of the probe beam forms an angle of 45° with the p-plane, i.e. the plane formed by the beam itself and the sample normal. Beyond the sample, the probe beam crosses a Soleil-Babinet compensator, a second polarizer at 90° with respect to the first one and finally a photodiode detector. Before being exposed to the intense light beam, the sample is optically isotropic and no intensity from the probe beam can be detected. In the presence of a light-induced birefringence, the sample will act as a retardation plate and, as described in the following sections, the intensity detected by the photodiode will be a function of the birefringence. The compensator is used to adjust the relative phase difference between the s and the p polarizations in order to obtain the sign of the birefringence. In the experiments described in this article, the polarization of the writing beam is at 45° with respect to the p-plane. However, results do not change if other polarizations are used.

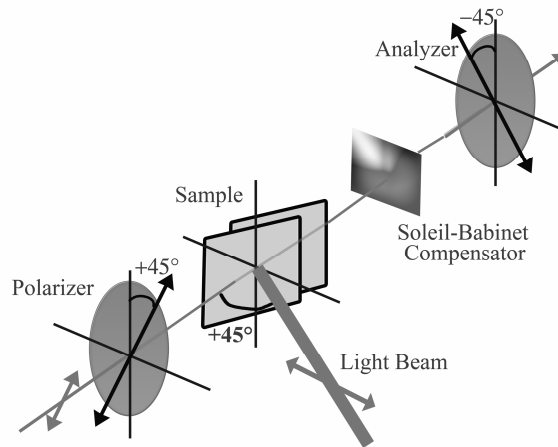


Fig. 2. The experimental set-up used to measure light-induced birefringence in the nanocrystalline dispersions of AZPON in a polyisobuthylmethacrylate matrix.

2.3 Transient current measurements

Evidence for charge photogeneration with no applied electric field was obtained by a transient current measurement method. Samples were connected to a power supply, with a resistor R (much lower than the internal resistance of the sample) in series. An oscilloscope was used to measure the voltage drop across the resistor, which is proportional to the current passing in the circuit. In our experiments $R = 1 \text{ M}\Omega$ was used, while the resistance of the samples was always higher than $100 \text{ M}\Omega$. Samples were illuminated and, after the light was turned off, an electric field was applied while monitoring the current flow with the oscilloscope. The delay between the light turn-off and the field turn-on ranged between a few ms and 1 hr. The light source was a He-Ne laser at $\lambda = 633 \text{ nm}$ and the intensity of the beam was around 1.5 W/cm^2 . Exposure times ranged between a few hundred ms and several minutes and the intensity of the applied field was $E = 5 \text{ V}/\mu\text{m}$.

2.4 Two-beam coupling experiments and phase shift measurements

Two Beam Coupling experiments were performed by overlapping on the sample two coherent p-polarized laser beams generated by a He-Ne laser at $\lambda = 633 \text{ nm}$. The diameter of each beam was $d \sim 0.8 \text{ mm}$ and their intensity $I = 0.4 \text{ W/cm}^2$. The sample normal was in the direction of the bisector of the two beams and the angle between beams was set in order to obtain an interference periodicity $\Lambda = 3 \mu\text{m}$. In such experimental conditions, given that the refractive index modulation must be lower than the measured birefringence (10^{-3}) and considering that samples were $50 \mu\text{m}$ thick, all experiments were carried out in the Bragg diffraction regime [20]. The intensities of the beams after they crossed the samples were monitored by two photodiode detectors and the gain coefficient Γ was calculated using $\Gamma d = \cos \alpha \ln[b\gamma/(b+1-\gamma)]$ where α is the internal angle between the sample normal and the beams, $\gamma = I_{\text{probe}}(I_{\text{pump}} \neq 0)/I_{\text{probe}}(I_{\text{pump}} = 0)$ is the amplification factor, d the sample thickness and b is the beams intensities ratio. Phase shift measurements as a function of the applied electric field were carried out using the same experimental set-up, but with the sample normal at 60° with respect to the bisector of the two beams. The experiment was performed by monitoring the intensities of the two beams while the exposed sample was translated at a constant speed along the grating direction. To avoid overlapping of different gratings, the translation time was much shorter than the grating formation time.

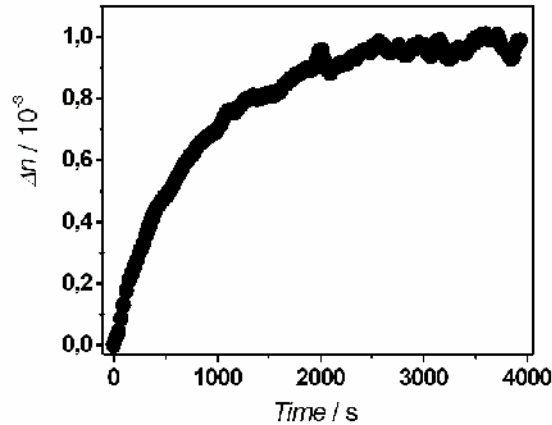


Fig. 3. Time dependence of the induced birefringence in a 50 μm thick sample of AZPON:PIBMA = 3:2. The birefringence was obtained using Eq. (1).

3. Results and discussion

3.1 Light-induced refractive index modulation

The absorption properties of AZPON in solution are illustrated in Fig. 1. AZPON dispersions were prepared by using a phase separation method, as described in the experimental section. In all experiments illustrated in this article, the composition of samples was kept constant at an AZPON:PIBMA = 3:2 wt ratio. This concentration corresponds to the highest nanocrystals content that it is possible to obtain while maintaining their size below the scattering limit in the visible: the resulting samples are absorbing but scattering is negligible. TEM shows brick-like crystalline domains shapes. The effect of illumination with a single beam at $\lambda = 633 \text{ nm}$, where the absorption coefficient is $\alpha = 113 \text{ cm}^{-1}$, can be understood by measuring light-induced birefringence [21]. This can be done by using the set-up illustrated in Fig. 2: the sample is illuminated with an intense beam ($I \sim 1.5 \text{ W/cm}^2$) at normal incidence and by a much weaker probe beam, with an intensity ~ 5 orders of magnitude lower. The probe beam is polarized at 45° with respect to the p-plane, defined by the probe beam itself and the sample normal, which in turn is rotated by 45° with respect to the probe beam. Beyond the sample, light from the probe beam crosses a Soleil-Babinet compensator and then another polarizer, crossed with respect to the first one. If an anisotropy in the refractive index of the material is induced during illumination, the sample acts as a retardation plate and the intensity recorded by the detector changes according to Eq. (1)

$$I = I_{\max} \sin^2 \left(\frac{\pi d \Delta n}{\lambda} - \frac{\psi_{SB}}{2} \right), \quad (1)$$

where I_{\max} is the light intensity transmitted through the sample, d is the total optical path-length within the sample, λ is the light wavelength and ψ_{SB} is the phase retardation introduced by the compensator. The magnitude of $\Delta n = n_p - n_s$ can then be obtained, where n_p and n_s are the refractive indices for polarizations in the p and s planes, respectively, for the given direction of the probe beam. Considering the refractive index of the unexposed sample (estimated at $n \sim 1.61$ from total reflection measurements) and the adopted geometry with an incidence angle in air $\theta_i = 45^\circ$, the measured Δn is about 80 % of the total induced birefringence: results are illustrated in Fig. 3. As no photoinduced birefringence could be

detected in the same experiment carried out on samples with a lower (30 %) AZPON content, where nanocrystals are not present [19], the first conclusion that can be drawn from such data is that light alone can reorient the crystalline domains, without having to use an applied field. This is remarkable, especially if we consider that similar values of birefringence (10^{-3}) can be reached by chromophore (molecular dipole) reorientations only for very high applied electric fields, of the order of several tens of $V/\mu\text{m}$. However, the effect is slow, as birefringence increases with a time constant $\tau \sim 10^3$ s. Assuming that nanocrystals are completely reoriented by light, we can estimate that the refractive indices of AZPON itself lay within a 10^{-3} range above and below the average value $n \sim 1.61$.

The light-induced reorientation is also evident when samples previously exposed to non-uniform illumination are placed between crossed polarizers and examined at the optical microscope. Fig. 4 is a picture of what is observed with a sample exposed to the interference pattern of two coherent light beams at $\lambda = 633$ nm. A pattern of induced birefringence with the same periodicity of the interference pattern ($\Lambda = 10$ μm , in this case) is clearly evident. The light/dark pattern is stable for days (and still evident after weeks) at room temperature and it is not observed if the sample is not placed between crossed polarizers, confirming the orientational nature of the light-induced effect.

There is experimental evidence indicating that the reason for the behaviour described above can be found in the photoconducting properties of the material used, as it will be discussed in the following. Light is absorbed as it travels through the sample and photogeneration is stronger on the side of the incoming light, producing an internal longitudinal (i.e. along the direction of propagation of light) electric field. In fact, the photorefractive and photoconducting properties of the AZPON/PIBMA mixture have been already reported [17-19]. However, such behaviour was previously investigated in the

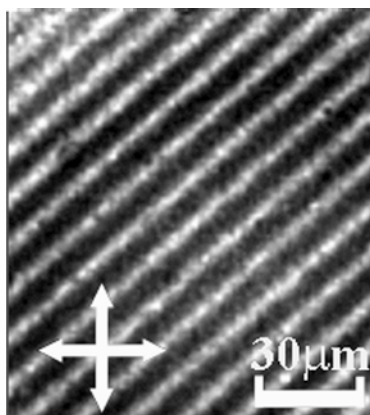


Fig. 4. Optical microscope picture of a 50 μm thick sample of AZPON:PIBMA = 3:2 previously exposed to the interference pattern generated by two beams at $\lambda = 633$ nm with a periodicity $\Lambda = 10$ μm . The sample is placed between two crossed polarizers, whose orientations are indicated by the arrows.

presence of an applied electric field, as usual in organic materials, where charge photogeneration efficiency is otherwise extremely low. Since in the experiments described here the birefringence is induced without applying a field, evidence of charge photogeneration when no field is applied is important and it was obtained by a transient current method. In such experiments, samples are first illuminated and then a field is applied in the dark to measure the current flow, as described in the experimental section. A difference in current between exposed and non-exposed samples can be detected only during the initial stages of

current flow, corresponding to the non-steady state current transients through the circuit. Results of current transients are shown in Fig. 5 for both exposed and non-exposed samples: a higher peak current is evident in the exposed samples. Results are reproducible and independent from sample history and exposure time to light, for illumination times t_1 between a few hundred ms and several minutes. In addition, the value of the peak current is independent from the time t_2 elapsed between the end of exposure and the measurement of currents, for elapsed times t_2 between a few ms and one hour. Although they are only qualitative and do not constitute a solid proof of photoconductivity, these results clearly indicate that in these materials light can generate charge carriers without the assistance of an electric field. Moreover, a portion of these carriers survives for a long time after light exposure, indicating the presence of deep traps, i.e. charge traps with energy barriers for mobility above $k_B T$ at room temperature. This is not surprising, given the fact that the material under investigation is a composite with a high concentration of interfaces, usually associated with charge trapping. Photogeneration in the absence of an applied electric field is certainly not new in organics, as it is present in organic photovoltaic devices and it was claimed (but never directly measured) to explain the photorefractive behaviour of a number of organic materials [12,13,16,22,23] usually poled and/or based on azo dyes. Here, besides presenting experimental evidence for photogeneration, the effect of the resulting electric field on the reorientation of nanocrystals is discussed.

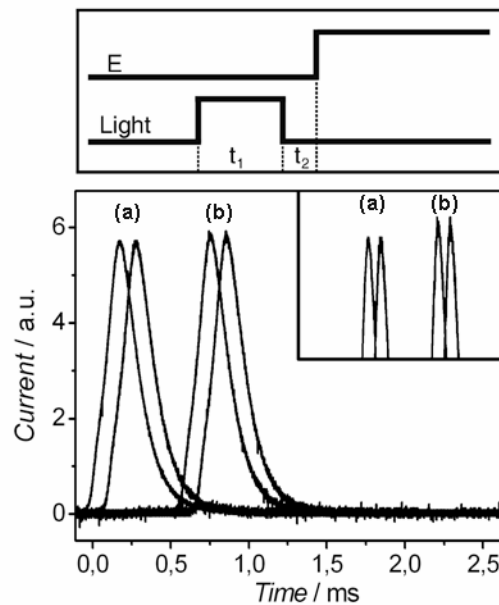


Fig. 5. Schematic illustration (upper part) of the experiment used to measure zero-field photo-induced charge generation in a $50\ \mu\text{m}$ thick sample of AZPON:PIBMA = 3:2. Samples are first illuminated for a time t_1 . After a time t_2 from the turn-off of the light, an electric field E is applied to measure the current. In the lower part, the transient current is shown for samples (a) kept in the dark (i.e. for $t_1 = 0$) and (b) pre-illuminated. In order to illustrate reproducibility, two examples of measurements are shown for both dark and pre-illuminated samples, each one translated on the time-scale for clarity. The inset is an enlargement of the peak currents.

In the following, we will describe some photorefractive properties of the AZPON/PIBMA nanocrystals, in order to better understand both their photogeneration properties and their refractive index modulation behaviour.

3.2 Photorefractive properties

Photorefractive performance is usually evaluated by two-beam coupling [7,8], in which two coherent writing beams interfere on the sample, excite charge carriers which move to dark regions and are trapped there, and the resulting space-charge field modulates the refractive index. As the photogenerated field is phase shifted with respect to the light pattern (unless it derives from a photovoltaic effect), so is the refractive index pattern and this is reflected in an asymmetric energy exchange between the two beams. Two-beam coupling experiments with and without an applied field have been carried out, as described in the experimental section, on the AZPON/PIBMA dispersions. The gain coefficient for two beams with the same polarization is given by:

$$\Gamma = \frac{4\pi}{\lambda} \delta n \sin \phi. \quad (2)$$

The measured gain was within $\Gamma = 70 - 90 \text{ cm}^{-1}$ range when no field was applied. In Eq. (2), λ is the light wavelength, ϕ is the phase shift between refractive index pattern and illumination and δn is the amplitude of the refractive index modulation.

One important feature of the energy exchange data is the time constant $\tau \sim 10^3 \text{ s}$ of the process, which is the same as in the light induced nanocrystal reorientation illustrated in Fig. 3: since photorefractivity is commonly interpreted in terms of reorientations induced by photogenerated fields, this is a further indication that the light-only induced reorientations in the AZPON/PIBMA composite are associated with photogenerated electric fields. It is interesting to compare the time-scale of the reorientations illustrated above (no field applied) with the timescale $\tau_E \sim 10^2 \text{ s}$ of the grating build-up when fields of the order of $10 \text{ V}/\mu\text{m}$ are applied [19]. The reorientation of the nanocrystals can be described as a process during which viscous and field torques are in equilibrium. Since AZPON does not possess any spontaneous polarization (its crystalline structure is centrosymmetric), the orientational energy per unit volume within an electric field can be written, assuming uniaxiality, as:

$$F_E = -\frac{1}{2} \epsilon_0 \Delta \epsilon E^2 \cos^2 \theta, \quad (3)$$

where $\Delta \epsilon$ is the dielectric anisotropy (the difference between the two different non-vanishing values in the diagonalized dielectric constant tensor), E the applied field and θ is the angle between the field and the uniaxial symmetry axis. The dielectric torque (per unit volume) will then be:

$$\Gamma_E = -\frac{1}{2} \epsilon_0 \Delta \epsilon E^2 \sin(2\theta). \quad (4)$$

During reorientation, such torque will work against dissipation at the interface between the nanocrystal and the polymer. Neglecting the shape-factor of the crystal, the viscous torque per unit surface can be written as

$$\Gamma_V = -\gamma \frac{d\theta}{dt}, \quad (5)$$

where γ is the polymer viscosity and l is the thickness of the polymer layer affected by the crystal reorientation. By equating torques, the time evolution of the reorientation can be easily obtained:

$$\operatorname{tg} \theta = \operatorname{tg} \theta_0 \exp\left[-\frac{\varepsilon_0 \Delta \varepsilon E^2 V}{\gamma S} t\right], \quad (6)$$

where θ_0 is the initial orientation of the crystal when the field is first applied, V is the crystal volume and S is the surface of the interface between the crystal and the polymer. The time constant of the reorientation scales then with the inverse of the second power of the field:

$$\tau = \frac{\gamma S}{\varepsilon_0 \Delta \varepsilon E^2 V}. \quad (7)$$

Since the time required for reorientation with an applied field $E \sim 10 \text{ V}/\mu\text{m}$ is $\tau_E \sim 10^2 \text{ s}$ and the time constant for the reorientation due to the light-induced field (no applied field) is $\tau_0 \sim 10^3 \text{ s}$, from Eq. (7) we can estimate a light-induced field $E_L \sim 3\text{-}4 \text{ V}/\mu\text{m}$.

The phase shift ϕ between the light pattern and the refractive index modulation has been measured by using the moving grating technique, as described in the experimental section (see Fig. 6). A value of $\phi = \pi/2$ was obtained with no applied field for two beams of comparable intensities. For beams of different intensities instead, the phase shift was lower, confirming the presence of a component of the light-induced electric field in the direction of the grating wavevector [7,8]. Similar experiments using applied fields of different polarities have also been carried out, with a slanted geometry (in order to obtain a component of the applied field along the grating wavevector), where the sample normal was tilted by 60° with respect to the beams bisector. Results as a function of the applied field intensity are shown in Fig. 6 (a). As expected, at high fields the phase shift is of different sign for different field polarities, corresponding to a gain of different sign. It is interesting to consider the phase data for the electric field polarity corresponding to a change of sign at high fields (circles in Fig. 6 (a)): for an applied field $E \sim 6 \text{ V}/\mu\text{m}$ the phase shift vanishes, while the index modulation does not (it is a monotonically increasing function of the applied field). Given the relative orientation of sample and writing beams, in these conditions the component of the applied field in the grating wavevector direction is $E_G \sim 3 \text{ V}/\mu\text{m}$. Since the phase shift is zero, one can assume that an applied field $E \sim 3 \text{ V}/\mu\text{m}$ is necessary to exactly counteract the effect of the light-generated electric field: this is in remarkable agreement with the estimation of the intensity of the light-induced field obtained above, from the measurement of the time constant of the light-induced reorientation (Eqs. 3-7).

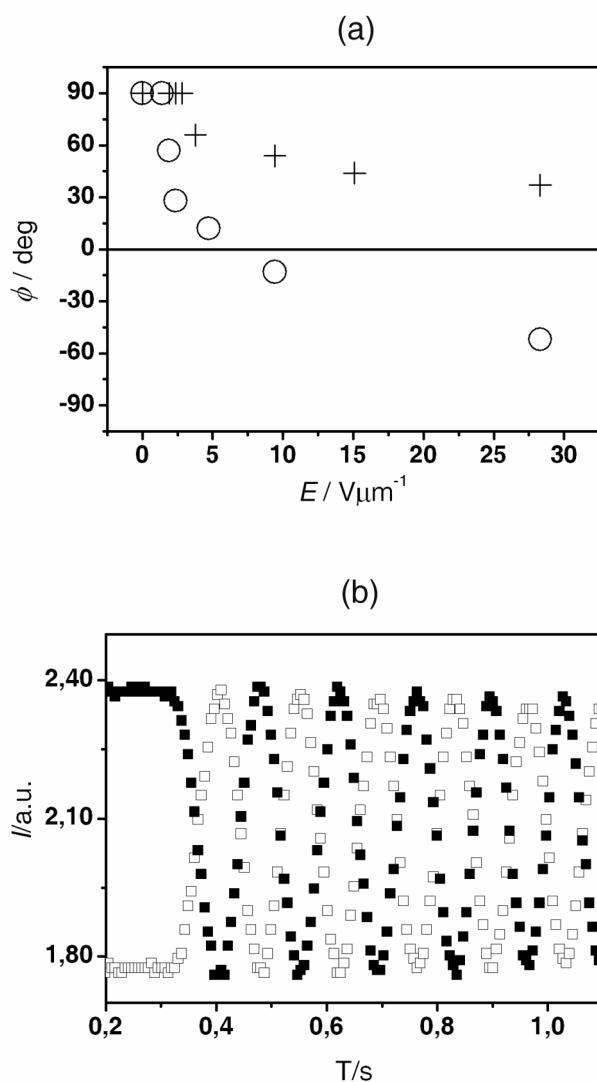


Fig. 6. (a) Applied electric field dependence of the phase shift between interference fringes and refractive index modulation in 50 μm thick samples of AZPON:PIBMA = 3:2. The two different symbols indicate fields of different polarity. (b) Typical variation of the light intensities of the two beams during a displacement of an exposed sample along the grating wavevector. The displacement started at a time $t = 0.3$ s. No electric field was applied.

4. Conclusion

In this work, the effectiveness as a light-responsive medium of a material with a morphology consisting of a dispersion of nanocrystals was assessed. By homogeneous illumination, a birefringence $\Delta n \sim 10^{-3}$ was induced in a dispersion of nanocrystals of AZPON within an amorphous polymer, without the application of an electric field. Refractive-index modulation upon inhomogeneous illumination with light was also observed. This modulation exhibits an anisotropy, visualised via the optical polarization microscope, i.e. it is an anisotropic grating. The birefringence was related to the reorientation of the crystals induced by a photogenerated

electric field. Evidence for charge-carrier photogeneration when no electric field is applied was obtained by electric current measurements under homogeneous illumination. The intensity of the light-induced electric field has been estimated by comparison with experiments on photorefractive behaviour carried out with applied fields: considering both the grating build-up time and the applied field dependence of the phase shift, a value for the photogenerated field $E \sim 3 \text{ V}/\mu\text{m}$ was obtained. The time required for the reorientation of the nanocrystals used in this study is long, as the birefringence grows with a time constant $\tau_0 \sim 10^3 \text{ s}$. Using a torque balance derivation, this time constant was found to depend on several parameters, see Eq. (7). In order to increase the speed of the effect (i.e. in order to decrease τ_0) it seems unrealistic to be able to somehow increase the intensities of the photogenerated fields beyond values of a few $\text{V}/\mu\text{m}$. Future work aiming at a faster effect should then concentrate on using nanocrystals with a higher dielectric anisotropy and on decreasing the viscosity at the crystal/polymer interface, by controlling the shape of the crystalline domains and/or by suitably treating their surface. Further experimental work aimed at understanding the molecular origin of the good charge photogeneration properties of AZPON and of similar complexes is in progress.

Acknowledgments

This work has been supported by MiUR under the project “Molecular and Organic/Inorganic Hybrid Nanostructures for Photonics” FIRB 2001 and through the Centro di Eccellenza CEMIF.CAL.